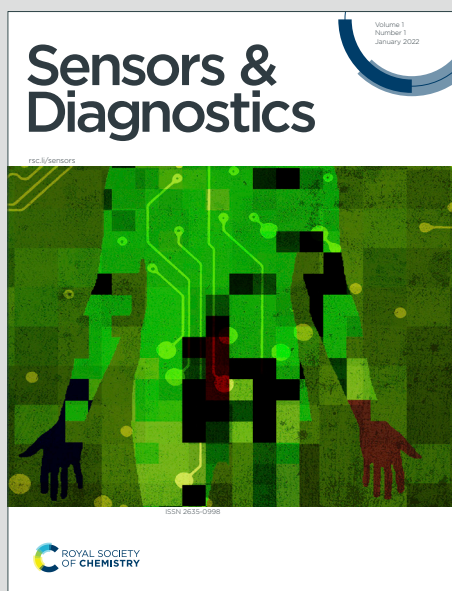


# Sensors & Diagnostics

Accepted Manuscript

This article can be cited before page numbers have been issued, to do this please use: S. Mondal and N. Dey, *Sens. Diagn.*, 2025, DOI: 10.1039/D5SD00232J.



This is an Accepted Manuscript, which has been through the Royal Society of Chemistry peer review process and has been accepted for publication.

Accepted Manuscripts are published online shortly after acceptance, before technical editing, formatting and proof reading. Using this free service, authors can make their results available to the community, in citable form, before we publish the edited article. We will replace this Accepted Manuscript with the edited and formatted Advance Article as soon as it is available.

You can find more information about Accepted Manuscripts in the [Information for Authors](#).

Please note that technical editing may introduce minor changes to the text and/or graphics, which may alter content. The journal's standard [Terms & Conditions](#) and the [Ethical guidelines](#) still apply. In no event shall the Royal Society of Chemistry be held responsible for any errors or omissions in this Accepted Manuscript or any consequences arising from the use of any information it contains.

# Engineering Anthraimidazoledione Charge-Transfer Fluorophores for Phospholipid Detection through Self-Assembly-Induced Emission

Sourav Mondal and Nilanjan Dey\*

Department of Chemistry, Birla Institute of Technology and Science Pilani, Hyderabad campus, Telangana-500078, India

\*Email: [nilanjan@hyderabad.bits-pilani.ac.in](mailto:nilanjan@hyderabad.bits-pilani.ac.in)

View Article Online

DOI: 10.1039/D5SD00232J

## ABSTRACT

Herein, we report the design and synthesis of anthraimidazoledione-based fluorescent probes for the selective detection of cardiolipin (CL) at pH 7.0 in PBS buffer (Phosphate buffered saline). Compound 1, bearing a protonated tertiary amine moiety, exhibited a strong turn-on fluorescence response upon interaction with CL, with a rapid response time (<15 s) and a detection limit of 5.8 nM. The probe also demonstrated high selectivity over other mitochondrial lipids and biomolecules, with minimal background interference. Also, the sensitivity towards CL was found to be dependent on the nature of the positively charged residue at the terminal position. Mechanistic studies revealed electrostatic complexation between the cationic probe and CL, supported by a 2:1 binding stoichiometry, increased anisotropy (0.147 → 0.595), and extended fluorescence lifetime ( $\tau = 2.78$  ns). These features highlight the potential of the probe for sensitive CL quantification and diagnostic applications.

## INTRODUCTION

In eukaryotic cells, lipids are vital for maintaining cellular function. Their amphipathic nature enables bilayer formation, which not only separates the cell from its environment but also compartmentalizes internal organelles. [1] Beyond structure, lipids serve as energy stores and signaling molecules in various cellular pathways. Cardiolipin (CL), a diphosphatidylglycerol lipid found exclusively in the inner mitochondrial membrane, plays a key role in electron transport and oxidative phosphorylation (**Fig. 1c**). [2] Comprising four unsaturated acyl chains and a doubly negative head group, CL modulates enzyme activity and interacts with cytochrome c (cyt c) to activate its peroxidase function, initiating mitochondrial apoptosis. During apoptosis, CL levels and distribution shift, impacting ATP synthesis, cyt c release, and ROS production. [3] CL depletion is associated with aging, Barth syndrome, and mitochondrial diseases like ischemia-reperfusion injury, gliomas, and cardiac failure. Conversely, CL overproduction occurs in Tangier disease. [4] Dysregulated CL metabolism is also linked to Parkinson's, HIV-1, and cancers, making it a critical biomarker. [5]

However, the specific detection of CL among structurally similar phospholipids remains challenging. Advanced techniques such as lipidomics profiling via high-resolution LC-MS offer quantitative analysis of CL with excellent sensitivity and specificity. [6] Nevertheless, these methods demand expensive instrumentation and skilled personnel, limiting widespread use. In contrast, optical detection, particularly fluorescence-based approaches, offers simplicity, accessibility, and high sensitivity. One of the earliest fluorescent dyes used for CL detection is 10-N-nonyl acridine orange (NAO), introduced in the early 1980s for mitochondrial staining. [7] NAO exhibits green fluorescence that diminishes upon interaction with CL. However, its utility for quantitative analysis is limited. The excitation and emission maxima of NAO are concentration-dependent, and a linear fluorescence response is achieved



only when the NAO/CL molar ratio is exactly 2:1. Additionally, NAO suffers from a small stokes shift, poor aqueous solubility, and an unclear mechanism of action, limiting its reproducibility and optimization potential. Despite these shortcomings, NAO remains in use due to the lack of suitable alternatives and the absence of a standardized protocol for CL detection.

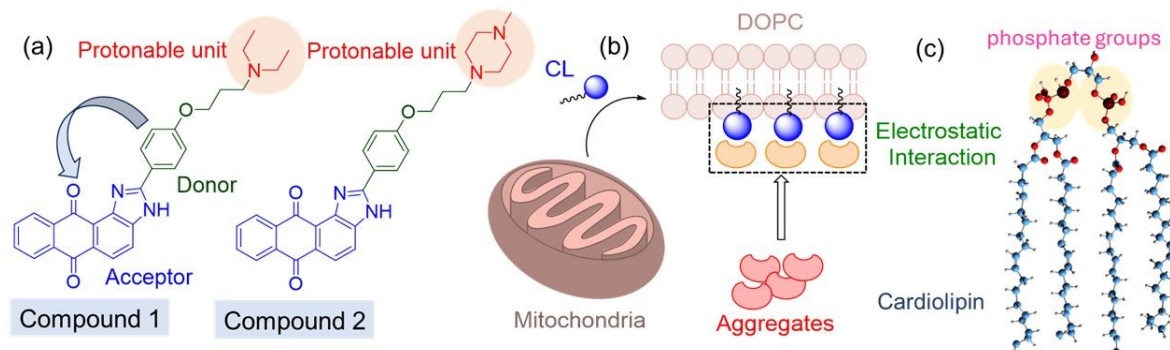


Figure 1. (a) Chemical structures of anthraimidazoledione-based charge transfer probes. (b) The schematic diagram shows binding of cationic probes with CL-doped DOPC vesicles. (c) Structure of cardiolipin (CL) with negatively-charged phosphate groups (highlighted).

Very recently, Tang et al. reported a Tetraphenylethene-based AIE active fluorescent probe for the detection of cardiolipin in aqueous medium. [8] Although the probe exhibited excellent sensitivity toward cardiolipin (CL), the observed emission changes were centered around  $\sim 480$  nm, resulting in a cyan fluorescence response. Considering this, herein we have developed anthraimidazoledione-based charge transfer probes that can show highly specific turn-on fluorescence response (red) upon interaction with CL at pH 7.0 in PBS buffer. The response towards CL was found to be rapid ( $< 15$  s) as well as sensitive (LOD: 5.8 nM), suitable for clinical diagnosis. The mechanistic studies indicated that electrostatic complexation between cationic probe and CL molecules could provide a rather rigid microenvironment (**Fig. 1b**), which substantially reduces the extent of non-radiative decay and results in turn-on fluorescence response.

## MATERIALS AND METHODS

All chemicals and reagents were purchased from reputable commercial vendors and used without further purification. The buffer solution was prepared according to standard procedures. Fluorescence measurements were performed using a Shimadzu RF-6000 spectrofluorometer with the excitation wavelength set at 505 nm and both excitation and emission slit widths maintained at 5.0 nm. All measurements were conducted in triplicate to ensure reproducibility, and the corresponding error bars were showed in the plots. Further details of the instrumental parameters and materials were mentioned in the supporting information file.

## RESULTS AND DISCUSSION

Design and synthesis of probe molecules: The synthesis of compounds 1–3 follows a convergent strategy starting from 1,2-diaminoanthraquinone, which undergoes an oxidative cyclocondensation reaction with various substituted aldehydes bearing functionalized phenyl rings. [9] The structure of the two probes (1 and 2) was shown above (**Fig. 1a**). The phenyl



rings in each case are pre-functionalized with diverse substituents such as diethylamino, piperazine, or carboxylic acid groups, connected via aliphatic linkers (**Fig. 1a**). This flexible hydrophilic functional groups with protonable terminal ends will give the molecules amphiphilic characteristics with improved water solubility, and enhanced biocompatibility. Anthraimidazolediones offer several compelling advantages as dye scaffolds and biosensors, including their planar  $\pi$ -conjugated backbone, which promotes strong visible-range absorption and fluorescence emission, and their intrinsic photostability and chemical robustness under thermal and physiological conditions.[10] These properties are further enhanced by electron-donating substituents, which induce intramolecular charge transfer (ICT), enabling high sensitivity to environmental polarity changes and facilitating the detection of biomolecular targets.[11] The presence of modifiable peripheral groups also allows for selective interactions with biomolecules, such as nucleic acids, proteins, and metal ions, making these dyes highly promising for bioimaging, diagnostic assays, and environmental sensing.

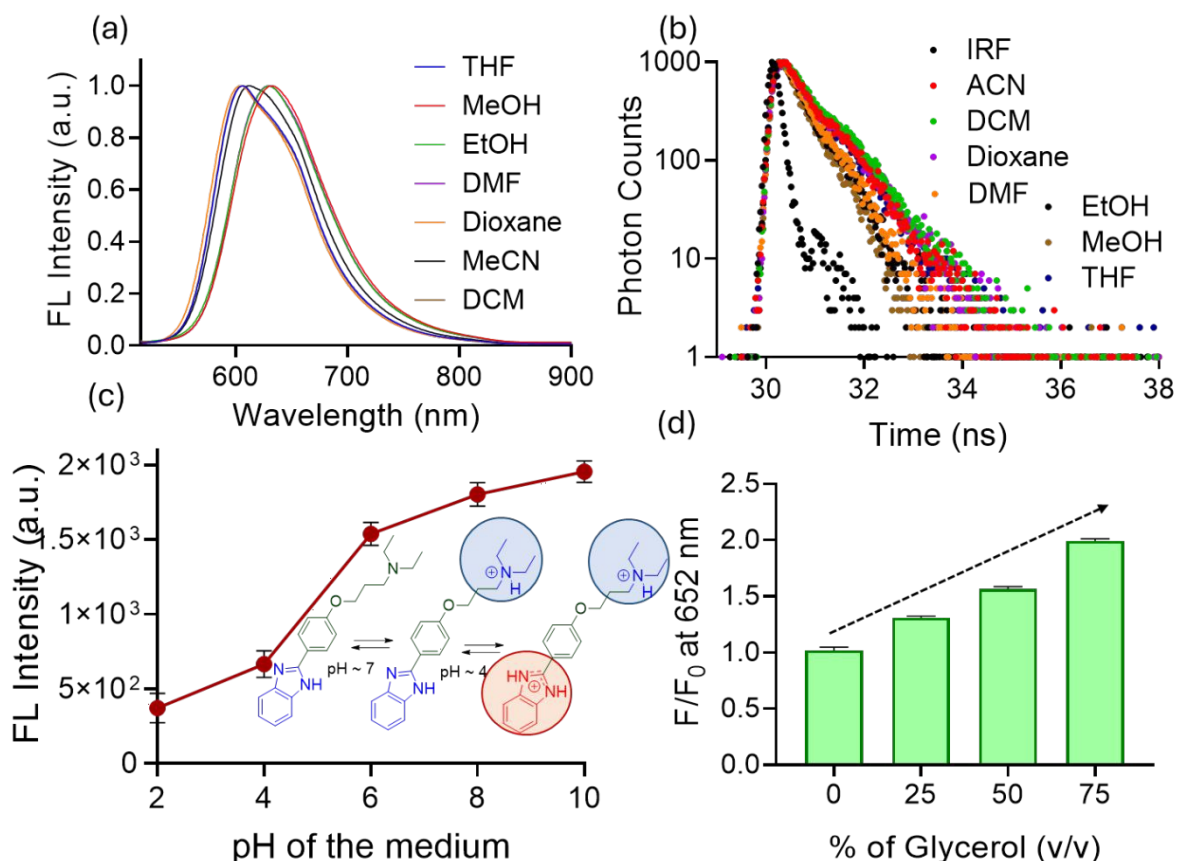


Figure 2. (a) Fluorescence spectra of 1 (10  $\mu$ M,  $\lambda_{ex}$  = 505 nm) in different organic solvents. (b) Time-dependent fluorescence spectra (TCSPC) of 1 (10  $\mu$ M,  $\lambda_{ex}$  = 505 nm) in different organic solvents at respective emission maxima. (c) Changes in fluorescence intensity as well as  $\lambda_{max}$  of 1 (10  $\mu$ M,  $\lambda_{ex}$  = 505 nm) at different pH conditions in buffered medium (d) Changes in fluorescence intensity of 1 (10  $\mu$ M,  $\lambda_{ex}$  = 505 nm) at 630 nm in different water-glycerol mixture medium (at pH 7).

Effect of solvent polarity on charge transfer characteristics: The fluorescence emission spectra of compound 1 recorded in different solvents exhibited pronounced solvatochromism (627 to 602 nm), clearly indicating its charge-transfer (CT) character (**Fig. 2a**). In nonpolar solvents



such as toluene and chloroform, the emission maxima are relatively blue-shifted, reflecting higher-energy emission due to poor stabilization of the excited CT state in a low dielectric environment. Conversely, in polar solvents such as acetonitrile, methanol, and DMSO, the emission maxima are significantly red-shifted as a result of enhanced stabilization of the CT excited state through solvent-dipole interactions and hydrogen-bonding effects, which lower the excited-state energy. This represents a typical case of positive solvatochromism associated with ICT fluorophores, where the Stokes shift increases progressively with solvent polarity because excitation is relatively insensitive to solvation, while the emission from the relaxed CT state is strongly stabilized in polar environments. The excitation spectra reinforced this behavior but showed much smaller solvent-dependent shifts, since the ground-state electronic distribution was expectedly less polar than the excited CT state, making ground-to-excited transitions less sensitive to solvent polarity. Overall, the absorption/excitation spectra remained relatively unchanged across solvents, whereas the emission spectra experienced dramatic polarity-dependent shifts, confirming that the probe operates via a solvent-stabilized CT mechanism (Fig. S1). In polar protic solvents such as methanol, additional hydrogen-bonding interactions also contributed to spectral broadening as well as partial quenching, adding complexity to the solvatochromic response.

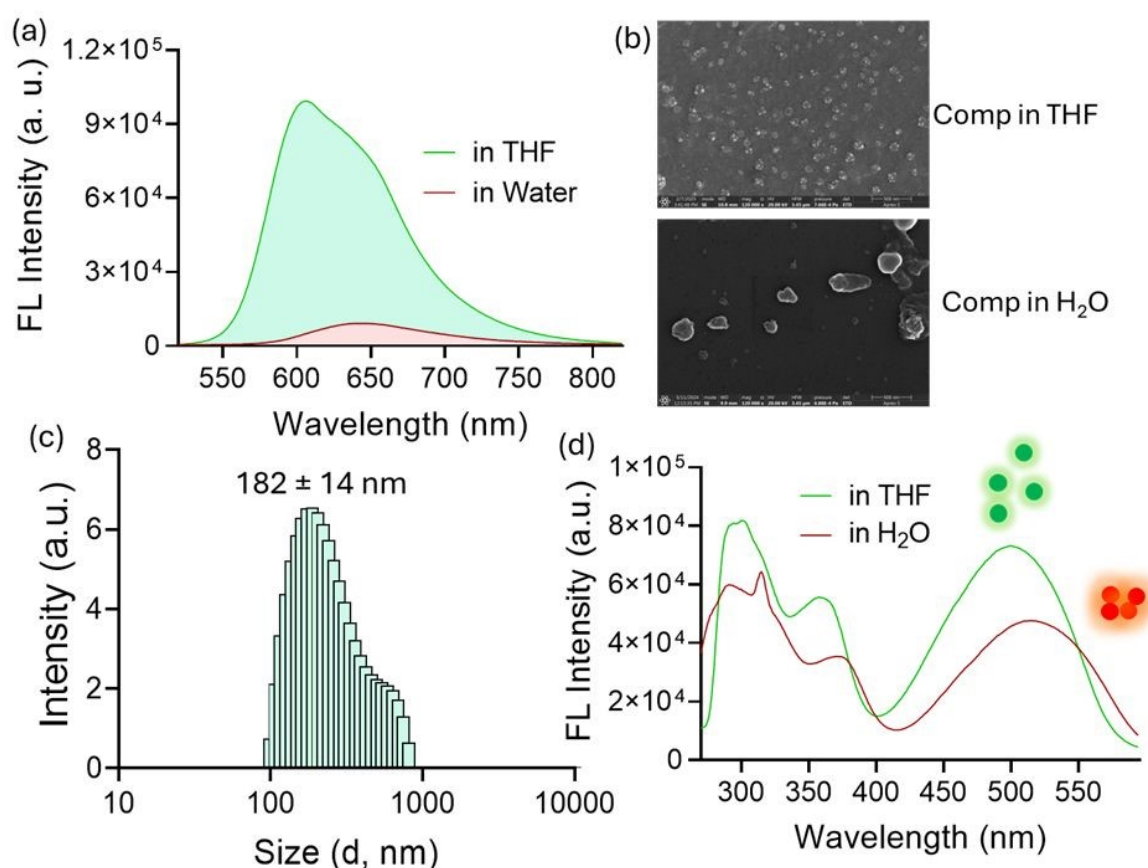


Figure 3. (a) Fluorescence spectra of 1 (10  $\mu$ M,  $\lambda_{ex}$  = 505 nm) in THF and PBS buffer (pH 7.0). (b) FESEM images of 1 in THF and water medium. (c) Determination of hydrodynamic diameter of 1 using DLS in buffered medium (pH 7). (d) Fluorescence excitation spectra of 1 in THF (605 nm) and buffered medium (630 nm) at pH 7.



The fluorescence lifetimes of **1** varied significantly across organic solvents, reflecting the interplay between solvent polarity, hydrogen bonding, and stabilization of the excited states (Fig. 1b). In non-protic and moderately polar solvents such as DCM, dioxane, THF, and MeCN, compound exhibited relatively longer lifetimes (0.54–0.63 ns) with bi-exponential decay behavior, indicating the coexistence of two emissive states, a locally excited (LE) state confined to the naphthalimide core and an intramolecular charge transfer (ICT) state arising from electron donation by the imidazole moiety to the naphthalimide acceptor (Table S1). In contrast, in more polar and hydrogen-bonding solvents such as DMF, EtOH, and MeOH, the fluorescence lifetime decreases markedly (0.37–0.43 ns) and becomes monoexponential, indicating dominance of a single emissive ICT state. The stronger solvent–solute interactions in these media stabilize the charge-separated excited state while simultaneously promoting non-radiative deactivation through internal conversion and hydrogen-bond-assisted quenching.

Self-assembly behaviour in the aqueous medium: Compound **1** in an apolar solvent like THF showed a fluorescence maximum at 605 nm, while in water (pH 7.0, PBS buffer), we observed poor emission intensity and a broad spectrum with a maximum centered at 654 nm (Fig. 3a). The fluorescence excitation spectra corresponding to the 605 and 654 nm bands exhibited distinct profiles (~20 nm red shift in the latter case) (Fig. 3d), indicating the presence of at least two different photoactive species in the reaction medium. Such ground-state heterogeneity might be attributed to a self-assembly process. [12] The dynamic light scattering (DLS) experiment suggested the formation of colloidal particles with an average hydrodynamic diameter of  $182 \pm 14$  nm (Fig. 3c). Further, FE-SEM image analysis confirmed formation of larger aggregates in the aqueous medium than that observed in THF (Fig. 3d). In PBS buffer, compound **1** showed shortest lifetime (~0.207 ns) with monoexponential decay. We believe that strong hydrogen bonding interaction enhanced non-radiative pathways, which along with aggregation possibly reduce the lifetime. The monoexponential nature of decay profile suggested complete quenching of LE contribution and dominance of a single, rapidly decaying ICT state (Fig. S2).

Effect of Microenvironment on the degree of self-association: The fluorescence response of the probe as a function of pH is governed by a delicate interplay between protonation–deprotonation equilibria, intramolecular charge transfer (ICT), and self-assembly behavior, involving the tertiary amine substituent (pKa ~9.0–9.5), the benzimidazole donor (pKa ~5.5), and the anthraquinone acceptor (Fig. 2c). At strongly acidic pH (2.0–4.0), both the benzimidazole and tertiary amine groups are protonated. Protonation of the tertiary amine site disrupts molecular packing and hinders self-assembly through electrostatic repulsions, while protonation of the benzimidazole diminishes its donor strength, suppressing ICT to the anthraquinone acceptor. Together, these effects resulted in destabilized aggregates and significantly quenched fluorescence. Around neutral pH (~6.0–8.0), near the benzimidazole pKa, the tertiary amine remains largely unprotonated (neutral), thereby favoring  $\pi$ - $\pi$  stacking and hydrogen-bonding interactions that stabilize self-assembled aggregates. At the same time, partial deprotonation of benzimidazole restores its donor capability, enabling efficient ICT to the anthraquinone acceptor. This dual reinforcement of ICT and aggregation would lead to maximum fluorescence intensity, with strong emission around 650–670 nm. At highly



basic pH (10.0), deprotonation of the benzimidazole NH would increase electrostatic repulsion between ionized groups, perturb conjugation, and disrupt aggregate packing, thereby enhancing nonradiative decay pathways and reducing emission intensity.

The fluorescence emission spectra of the probe in water and water-glycerol mixtures revealed a pronounced viscosity-dependent enhancement of emission, reflecting the interplay between intramolecular charge transfer (ICT) and restricted molecular motions (Fig. 2d). In pure water, compound 1 showed relatively weak fluorescence at ~654 nm due to efficient nonradiative decay pathways arising from free intramolecular rotations and solvation effects. Upon increasing the glycerol content (water-glycerol 1:1), the fluorescence intensity increased markedly, and in the highly viscous 1:4 mixture the emission was further amplified. This enhancement originated from the restriction of intramolecular motions (RIM) in viscous environments, which suppressed nonradiative relaxation and promoted radiative decay. At the same time, the presence of glycerol favoured  $\pi$ - $\pi$  stacking and hydrophobic interactions, stabilizing self-assembled aggregates that further boosted fluorescence through aggregation-induced emission enhancement (AIEE)-like effects. Together, these observations demonstrate that the probe exhibits strong viscosity-dependent fluorescence amplification, highlighting its potential as a microenvironment- and viscosity-sensitive ICT fluorophore.

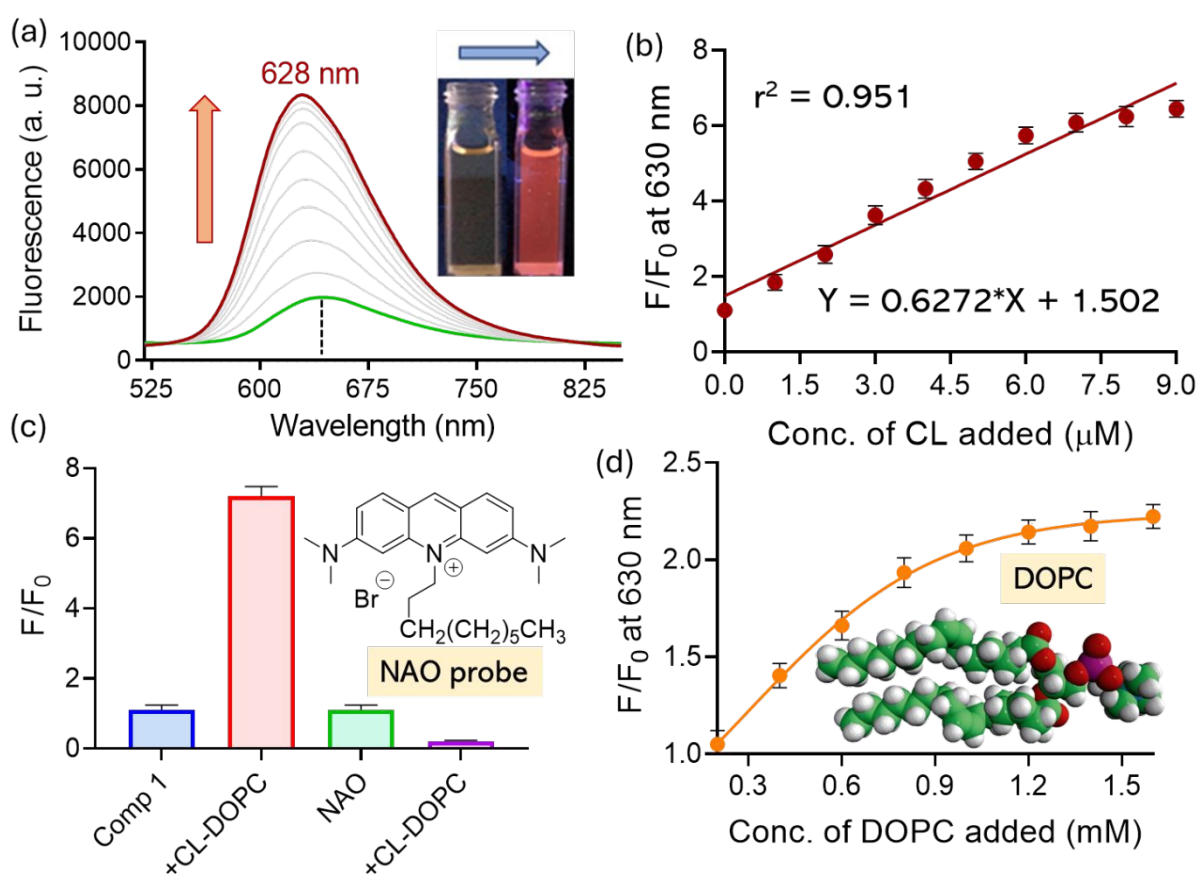


Figure 4. (a) Fluorescence titration of 1 (10  $\mu$ M,  $\lambda_{ex}$  = 505 nm) with CL-doped DOPC vesicles in PBS buffer (pH 7.0). (b) Changes in fluorescence intensity of 1 (10  $\mu$ M,  $\lambda_{ex}$  = 505 nm) at 602 nm upon addition of CL in PBS buffer (pH 7.0). (c) Changes in fluorescence intensity of 1 and NAO (10  $\mu$ M) upon addition of CL-doped DOPC vesicles in PBS buffer (pH 7.0). (d) Changes in fluorescence intensity of 1 (10  $\mu$ M) upon addition of CL (10  $\mu$ M)-doped DOPC (0.2 - 1.6 mM) vesicles in PBS buffer (pH 7.0).



Fluorometric analysis of cardiolipin: Subsequently, the fluorescence spectrum of compound 1 was recorded upon its incorporation into DOPC phospholipid vesicles at pH 7.0 in PBS buffer. In DOPC (1,2-dioleoyl-sn-glycero-3-phosphocholine), compound 1 exhibited relatively high emission intensity (~3.5-fold increase), with an emission maximum blue-shifted ( $\lambda_{em} = 645$  nm) compared to that observed in pure aqueous medium. This blue shift, along with improved quantum yield, indicates a relatively hydrophobic microenvironment around the probe molecules. [13] We then prepared various CL-doped DOPC vesicles (DOPC concentration 1 mM, CL = 0 to 0.01%), and the fluorescence spectra were recorded upon the addition of a fixed concentration of compound 1 (10  $\mu$ M) at physiological pH in a buffered medium. This concentration range was selected to match the physiological range of CL in the mitochondrial membrane. It was observed that with increasing CL content in the DOPC vesicles, the fluorescence intensity of compound 1 gradually increased (~7-fold) with a prominent blue shift from 645 to 627 nm (**Fig. 4a**). When the changes in fluorescence intensity ( $F/F_0$ ) of compound 1 at 630 nm were plotted against the CL concentration (0–10  $\mu$ M), a straight line with a linear regression coefficient > 0.99 was obtained (**Fig. 4b**). Unlike conventional NAO-based assays, compound 1 can achieve quantitative estimation of CL within the physiologically relevant dynamic concentration range. Notably, changes in the fluorescence intensity of compound 1 were observed immediately upon mixing with CL-containing vesicles, with no additional incubation time required – highlighting the suitability of the proposed fluorometric assay for rapid clinical diagnostics.

Fluorescence spectra of compound 1 were also recorded at different DOPC concentrations (0.2–1.6 mM) while keeping CL concentration fixed at 10  $\mu$ M (**Fig. 4d**). A modest enhancement in fluorescence intensity (~2.2-fold) was observed at higher DOPC levels. Thus, we deduced that CL is primarily responsible for the turn-on fluorescence response. Higher DOPC concentrations promote better vesicle formation, enabling more efficient partitioning of CL and facilitating enhanced interactions between the probe and CL-rich membrane domains. Additionally, an increase in DOPC likely expands the overall membrane surface area, offering more accessible sites for probe-CL interaction, even if the absolute CL concentration remains unchanged. [14]



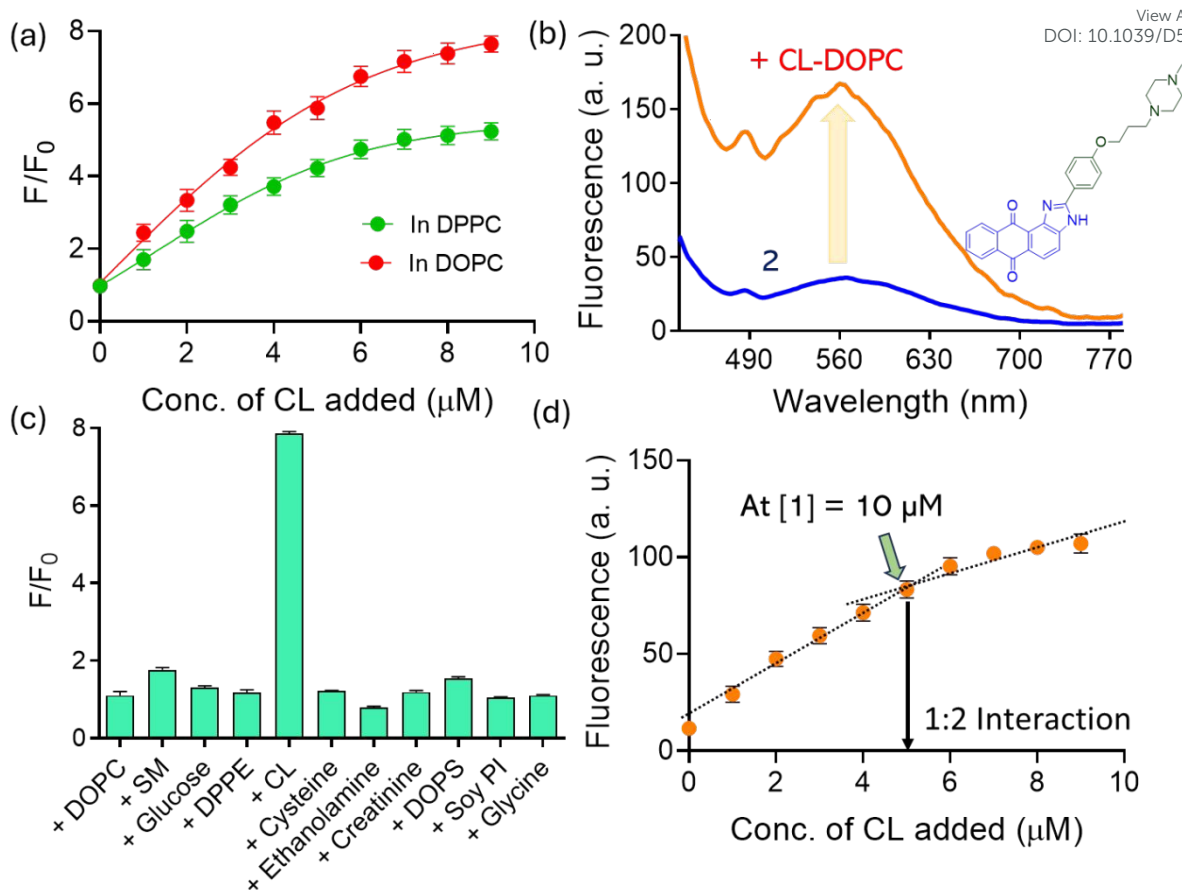


Figure 5. (a) Changes in FL intensity of 1 (10  $\mu\text{M}$ ,  $\lambda_{\text{ex}} = 505 \text{ nm}$ ) at 630 nm with CL-doped DOPC and DPPC (1 mM) vesicles in PBS buffer (pH 7.0). (b) Fluorescence spectra of 2 (10  $\mu\text{M}$ ,  $\lambda_{\text{ex}} = 505 \text{ nm}$ ) upon addition of CL (10  $\mu\text{M}$ )-doped DOPC in PBS buffer (pH 7.0). (c) Changes in fluorescence intensity of 1 (10  $\mu\text{M}$ ) at 630 nm upon the addition of different lipids and biomolecules doped in DOPC vesicles. (d) Changes in fluorescence intensity of 1 (10  $\mu\text{M}$ ,  $\lambda_{\text{ex}} = 505 \text{ nm}$ ) upon addition of CL (10  $\mu\text{M}$ )-doped DOPC (1 mM) vesicles in PBS buffer (pH 7.0).

Further, to examine the effect of the host lipid on CL sensing, we also investigated the interaction of compound 1 with CL doped into DPPC (1,2-dipalmitoyl-sn-glycero-3-phosphocholine) membranes by fluorescence titration. Unlike DOPC, which has a phase transition temperature around  $-17 \text{ }^\circ\text{C}$ , DPPC has a significantly higher transition temperature ( $\sim 41 \text{ }^\circ\text{C}$ ). Consequently, DOPC forms fluid-like membranes at room temperature, while DPPC remains in a solid, gel-like phase. Upon increasing CL concentration from 0 to 10  $\mu\text{M}$ , we observed only  $\sim 5$ -fold fluorescence enhancement in the DPPC system (Fig. 5a & S3). We believe the rigid, gel-like structure of DPPC restricts the mobility and accessibility of CL, resulting in less effective interaction with probe 1. In contrast, the fluid nature of DOPC facilitates stronger interactions between compound 1 and CL, allowing the probe to embed within the membrane and form stable electrostatic complexes. [15] We also tested another anthraimidazodione derivative bearing a terminal piperazine moiety for sensing studies. Like the tertiary amine group ( $\text{pK}_a \approx 10.7$ ), the piperazine unit ( $\text{pK}_{a1} \approx 9.5$ ;  $\text{pK}_{a2} \approx 5.6$ ) is expected to exist predominantly in its protonated form under aqueous conditions. [16] Upon interaction with CL, we observed  $\sim 5.5$ -fold fluorescence enhancement (Fig. 5b). The



comparatively weaker response of compound 2 may be due to the relatively lower basicity of the piperazine unit compared to the tertiary amine. According to the Henderson-Hasselbalch equation, ~99.9% of compound 1 is expected to remain in its protonated state at pH 7.0.

Interference studies: To confirm the selectivity of our system toward CL, we prepared DOPC vesicles doped with various biomolecules (glucose, cysteine, creatinine, urea, ethanolamine, glycine, etc.) under similar experimental conditions. When compound 1 was exposed to these vesicles under similar condition, no detectable change in fluorescence was observed. We also examined the response of compound 1 to other mitochondrial lipids such as DPPE (1,2-dipalmitoleoyl-sn-glycero-3-phosphoethanolamine), soy PI (1- $\alpha$ -phosphatidylinositol), DOPS (1,2-dioleoyl-sn-glycero-3-phospho-L-serine), and SM (N-hexanoyl-D-sphingomyelin) (**Fig. 5c**). In all cases, compound 1 showed a turn-on fluorescence response selectively in the presence of CL-doped DOPC membranes. Though DOPS and soy PI are negatively charged, they carry only one negative charge per molecule and constitute only 1% and 2% of the total mitochondrial membrane lipid content, respectively (CL contributes ~20%).<sup>[17]</sup> Thus, their low abundance is unlikely to interfere with the response of compound 1 toward CL. In contrast, the commercially available CL-sensitive fluorescent probe, 10-Nonyl acridine orange (NAO), showed ~4.3-fold fluorescence quenching upon exposure to CL (10  $\mu$ M) embedded DOPC vesicles (1 mM) (**Fig. 4c**). It is important to note that turn-on fluorescence probes are generally more advantageous than turn-off sensors due to higher signal-to-noise ratios and minimal background interference. Moreover, NAO was found to show significant interference from other lipids such as DPPE, soy PI, and DOPS.

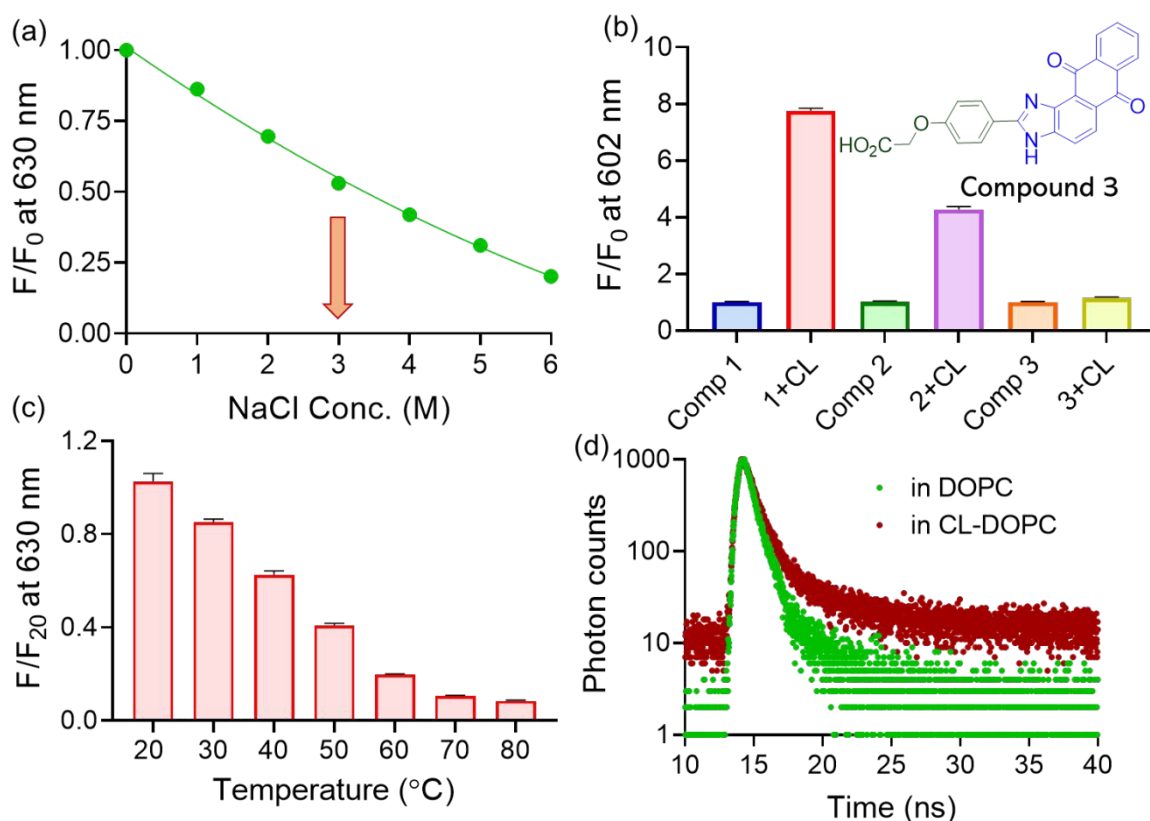


Figure 6. (a) Changes in FL intensity of 1 (10  $\mu$ M,  $\lambda_{ex}$  = 505 nm) in CL-doped DOPC (1 mM) vesicles in the presence of NaCl (0 – 6 M) in PBS buffer (pH 7.0). (b) Changes in fluorescence



intensity of 1, 2, and 3 (10  $\mu\text{M}$ ,  $\lambda_{\text{ex}} = 505 \text{ nm}$ ) upon addition of CL (10  $\mu\text{M}$ )-doped DOPC in PBS buffer (pH 7.0). (c) Changes in FL intensity of 1 (10  $\mu\text{M}$ ) in CL-doped DOPC vesicles at different temperatures. (d) Changes in fluorescence lifetime of 1 (10  $\mu\text{M}$ ,  $\lambda_{\text{ex}} = 505 \text{ nm}$ ) at 628 nm in DOPC (1 mM) vesicles with and without CL (10  $\mu\text{M}$ ).

**Mechanistic investigation:** We performed a series of spectroscopic studies to elucidate the mode of interaction between compound 1 and CL. Job plot analysis showed a peak at  $\sim 0.7$ , indicating a 2:1 binding ratio of compound 1 to CL (**Fig. 5d**). This matches their respective charge ratios and suggests that the interaction is primarily electrostatic in nature. To evaluate the stability of the ion-pair complex, we observed a gradual quenching of fluorescence with increasing NaCl concentration (0–6 M) (**Fig. 6a**), indicating competitive binding of  $\text{Na}^+$  ions with CL, leading to dissociation of the probe-lipid complex and release of free dye into solution.[18] When another anthraimidazoldione dye with a  $-\text{COOH}$  terminal (negatively charged) denoted as compound 3 was exposed to CL-containing DOPC vesicles, no detectable fluorescence enhancement was observed, confirming the importance of the positively charged tertiary amine in compound 1 for selective recognition (**Fig. 6b**). Temperature-dependent fluorescence measurements (20 to 80  $^{\circ}\text{C}$ ) of compound 1 in the presence of CL-containing DOPC vesicles showed a gradual decrease in emission intensity with increasing temperature (**Fig. 6c**). This suggests that thermal agitation may dissociate the preformed charge-pair complex. [19] Interestingly, the fluorescence excitation spectrum of compound 1 in CL-doped vesicles closely resembled that in organic solvents like THF (**Fig. S4**). This implies that electrostatic binding to CL reduces self-assembly, leading to the formation of monomeric or small aggregates. The DLS experiment was performed to analyze the particle size of DOPC vesicles with and without CL in the presence of compound 1. The average hydrodynamic diameter was found to be slightly smaller (from  $140.2 \pm 10.3$  to  $127.3 \pm 15.8 \text{ nm}$ ) when CL is present in DOPC vesicles (**Fig. S5**). This size reduction suggests a potential reorganization of the vesicle surface or tighter packing induced by electrostatic interactions between CL and the cationic probe (1).[20]

Due to electrostatic complexation, we observed an increase in fluorescence anisotropy values of compound 1 from 0.147 to 0.595 upon addition of CL-containing DOPC vesicles. In contrast, only a modest increase (0.147 to 0.208) was seen with DOPC vesicles alone (no CL), indicating enhanced conformational rigidity upon complex formation. [21] The electrostatic interaction between compound 1 and CL likely restricts rotational freedom and enhances anisotropy. Additionally, hydrophobic interactions may cause the probe to embed partially into the lipid membrane, further reducing its conformational flexibility. Lastly, fluorescence lifetime measurements at pH 7.0 in buffered medium revealed a monoexponential decay ( $\tau = 1.06 \text{ ns}$ ) in the presence of DOPC vesicles, while a biexponential decay with a significantly higher average lifetime ( $\tau = 2.78 \text{ ns}$ ) was observed in CL-doped vesicles (**Fig. 5d**). This suggests that CL binding induces a more rigid and stabilized environment around the probe, suppressing non-radiative decay and prolonging excited-state lifetime – consistent with our fluorescence anisotropy findings.[22]

CONCLUSION



In summary, we have developed a novel anthraimidazoledione-based fluorescent probe system for the highly selective turn-on fluorescence sensing of cardiolipin (CL) in aqueous environments under physiological conditions. The lead compound, bearing a terminal tertiary amine group, exhibited strong intramolecular charge-transfer (ICT) characteristics and demonstrated a significant fluorescence enhancement (~7-fold) with a blue shift in emission maximum from 635 nm (in water) to 602 nm upon interaction with CL-doped DOPC vesicles. The detection limit (LOD) was determined to be 5.8 nM, well within the physiologically relevant range of mitochondrial CL concentration. Notably, the probe responded instantly (<15 s) without requiring additional incubation or washing steps, offering a rapid readout ideal for diagnostic applications. Selectivity studies showed negligible fluorescence response in the presence of other biomolecules and mitochondrial lipids such as DOPS, DPPE, soy PI, and SM. Compared to the widely used dye 10-nonyl acridine orange (NAO), which showed a turn-off response (~4.3-fold quenching) and significant lipid interference, our probe displayed a superior turn-on mechanism, which ensures a better signal-to-noise ratio and lower background interference. Mechanistic investigations confirmed that the sensing event is driven primarily by electrostatic interactions between the cationic probe and anionic CL. Job plot analysis revealed a 2:1 binding stoichiometry, while fluorescence anisotropy increased markedly from 0.147 to 0.595, indicating a rigid, constrained microenvironment around the probe upon CL binding. A corresponding increase in fluorescence lifetime (from  $\tau = 1.06$  ns in DOPC vesicles to  $\tau = 2.78$  ns in CL-doped vesicles) further supports the formation of a stabilized probe-CL complex. These results underscore the promise of anthraimidazoledione-based fluorophores as next-generation optical sensors for real-time CL monitoring, with applications in mitochondrial research, disease diagnostics, and therapeutic screening.

## SUPPORTING INFORMATION

The data supporting this article have been included as part of the supplementary information (SI). The supporting information file includes the synthesis of the probes, experimental section, and additional spectroscopic data.

**AUTHOR CONTRIBUTIONS** **Sourav Mondal:** Writing – original draft, Visualization, Validation, Methodology, Investigation, Formal analysis. **Nilanjan Dey:** Writing – review & editing, Supervision, Resources, Project administration, Conceptualization.

## CONFLICT OF INTEREST

The authors declare that they have no known competing financial interests or personal relationships that could have appeared to influence the work reported in this paper.

## ACKNOWLEDGEMENT

ND thanks the Ministry of Education STARS [STARS-2/2023-0300] for the grants. The SM is thankful to BITS Pilani Hyderabad campus for all technical and financial support.

## REFERENCES

- [1] G. Van Meer, D. R. Voelker, G. W. Feigenson, *Nat. Rev. Mol. Cell Biol.* 2008, **9**, 112-124.



- [2] (a) G. Paradies, V. Paradies, V. De Benedictis, F.M. Ruggiero, G. Petrosillo, *Biochim. Biophys. Acta, Bioenerg.*, 2014, **1837**, 408-417. (b) A.T. Law, S.B. Adeloju, *Talanta.*, 2013, **114**, 191-203.
- [3] (a) S.L. Iverson, S. Orrenius, *Arch. Biochem. Biophys.*, 2004, **423**, 37-46. (b) D. K. Mal, H. Pal, G. Chakraborty, *Trends Anal. Chem.*, 2024, **171**, 117493.
- [4] E. Bertero, I. Kutschka, C. Maack, J. Dudek, *Biochim. Biophys. Acta Mol. Basis Dis.*, 2020, **1866**, 165803.
- [5] Y.Y. Zhao, H. Miao, X.L. Cheng, F. Wei, *Chem. Biol. Interact.*, 2015, **240**, 220-238.
- [6] S. S. Bird, V.R. Marur, M.J. Sniatynski, H.K. Greenberg, B.S. Kristal, *Anal. Chem.* 2010, **83**, 940.
- [7] S. Mondal, N. Dey, *J. Mater. Chem. B*, 2026, **14**, 1135-1149.
- [8] C.W. Leung, Y. Hong, J. Hanske, E. Zhao, S. Chen, E.V. Pletneva, B.Z. Tang, *Anal. Chem.*, 2014, **86**, 1263-1268.
- [9] P. Chaudhuri, H. K. Majumder, S. Bhattacharya, *J. Med. Chem.*, 2007, **50**, 2536-2540.
- [10] B. Chettri, A. Pal, S. Jha, N. Dey, *Dalton Trans.*, 2024, **53**, 6343-6351.
- [11] S. Pise, N. Dey, *Dalton Trans.*, 2025, **54**, 2896-2907.
- [12] R. S. Fernandes, N. Dey, *Ind. Eng. Chem. Res.*, 2023, **62**, 21536-21545.
- [13] S. Mondal, N. Dey, *ACS Appl. Polym. Mater.*, 2024, **6**, 10242-10253.
- [14] A. S. Reddy, D. T. Warshaviak, M. Chachisvilis, *Biochim. Biophys. Acta Biomembr.*, 2012, **1818**, 2271-2281.
- [15] F. Khalili, A. Henni, A. L. East, *J. Chem. Eng. Data.*, 2009, **54**, 2914-2917.
- [16] S. Mondal, C. -H. Chang, N. Dey, *ACS Appl. Nano Mater.* 2026, **9**, 2501-2513.
- [17] C. W. T. Leung, Y. Hong, B. Z. Tang, *Anal. Chem.*, 2014, **86**, 179-186.
- [18] R. A. Böckmann, A. Hac, T. Heimbürg, H. Grubmüller, *Biophys. J.* 2003, **85**, pp.1647-1655.
- [19] S. Patra, N. Dey, *Dalton Trans.* 2025, **54**, 5502-5510.
- [20] M. C. Stuart, E. J. Boekema, *Biochim. Biophys. Acta, Biomembr.* 2007, **1768**, 2681-2689.
- [21] A. Volpato, D. Ollech, J. Alvelid, M. Damenti, B. Müller, A. G. York, M. Ingaramo, I. Testa, *Nat. Biotechnol.* 2023, **41**, 552-559.
- [22] W. Wang, N. K. Wong, S. L. Bok, M. Zuo, C. M. Croix, G. Mao, A. Kapralov, H. Bayir, V. E. Kagan, D. J. Yang, *J. Am. Chem. Soc.* 2023, **145**, .11311-11322.



Engineering Anthraimidazole-dione Charge-Transfer Fluorophores for Phospholipid View Article Online  
DOI: 10.1039/D5SD00232J

Detection through Self-Assembly-Induced Emission

Sourav Mondal and Nilanjan Dey\*

Department of Chemistry, Birla Institute of Technology and Science Pilani, Hyderabad  
campus, Telangana-500078, India

\*Email: [nilanjan@hyderabad.bits-pilani.ac.in](mailto:nilanjan@hyderabad.bits-pilani.ac.in)

Data will be available from authors on reasonable request

